Biotemplated Synthesis of Metallic Nanoclusters Organized in Tunable Two-Dimensional Superlattices

D. Alloyeau, B. Stéphanidis, X. Zhao, E. Larquet, N. Boisset, C. Ricolleau

Biotemplated synthesis of metallic nanoclusters organized in tuneable 2D superlattices

D. Alloyeau[1,*], B. Stéphanidis[1,2], X. Zhao[1,2], E. Larquet[2], N. Boisset[2] and C. Ricolleau[1]

[1]Laboratoire Matériaux et Phénomènes Quantiques (MPQ), CNRS UMR 7162 / Université Paris Diderot – Paris 7, Bâtiment Condorcet, Case 7021, 75205 Paris Cedex 13, France
[2]Institut de Minéralogie et de Physique de la Matière Condensée (IMPMC), UMR CNRS 7590 – Université Paris 6, 4 place Jussieu, 75252 PARIS Cedex 05, France

[*] Corresponding Author
Email : Damien.alloyeau@univ-paris-diderot.fr, phone: +33 1 57 27 69 83

Abstract

Bio-templating has emerged as a very promising approach to produce inorganic materials organized into well-defined architectures. In this paper, we combined both biochemistry and physical approaches to control the size and 2D organization of metallic nanoparticles (NPs). We used self-assembled Tomoto Bushy Stunt Virus and streptavidin 2D crystals as biotemplates for the growth of silver NPs by thermal evaporation. On the one hand, the tuneable arrangement of the virus superlattices offers an unprecedented opportunity to control the NPs organization. On the other hand, 2D protein crystals allow the formation of perfectly periodic NPs arrays, with a sub-10 nm lattice parameter and a very narrow NPs size distribution. These two UHV-compatible biotemplates allow the formation of organized NPs assemblies over long distance, which are stable over time.

Keywords
Biotemplating, thermal evaporation, Tomoto Bushy Stunt Virus, Streptavidin protein, metallic nanoparticles.

1. Introduction

The control over the spatial organization of nano-objects is one of the prominent challenges of nanosciences. The fabrication of 2D-organized assembly of metallic, oxide or semiconductor nanoparticles (NPs) is attracting increasing attention because of the technological potential that arises from the control of cluster interactions. Indeed, the design of 2D-organized NPs assembly with well defined environment and inter-particle distances offers an unique opportunity to tune the overall properties of the materials [1,2].

Bottom-up fabrication techniques are being explored because they provide the ability to control the organization of materials on smaller length scales that top-down methods. Among the bottom-up techniques, the spontaneous organization of chemically-prepared NPs controlled via weak surface interactions, is a method of choice to form well-defined nano-arrays [3]. The possibility to pattern NPs by using vapor phase deposition on vicinal surfaces is also frequently utilized [4]. More recently, the bio-nanofabrication has emerged as a very encouraging approach to produce inorganic materials organized into well-defined architectures [5]. Several self-assembled structures derived from biological systems such as DNA [6], viruses [7], ferritin [8], or two dimensional protein crystals [9-11] have been used as biotemplates to induce the formation of NP arrays. However, because of the ultra-high vacuum (UHV) conditions required by the fabrication of NPs using physical methods (i.e. thermal evaporation [12] or pulsed laser deposition [13-15]...), chemically-prepared NPs are generally used on biological nanostructured surfaces. In the present work, we used 2D self-organized Tomoto Bushy Stunt Viruses (TBSV) and streptavidin 2D crystals, as nanopatterned substrates for the growth of metallic NPs by thermal evaporation. These UHV-compatible biotemplates are a promising alternative route to produce and control self-assembled NP patterns over long distance, since physical nanofabrication methods allow a very fine control over the quantity and the flux of deposited matter or eventually the composition of multi-element particles.

2. Experimental section

The 2D arrays of TBSV virus are obtained using the method known as the microdrop on mica [16-18]. This technique is perfectly adapted to the fabrication of 2D organization of macromolecules like viruses. Its principle is simple: it consists in depositing, on a sheet of mica, one micro-drop of a diluted solution containing viruses to which a condensing medium were added.

TBSV were stored as high concentration (19 mg/ml) at 4°C and diluted to an appropriate concentration immediately before use. Compact TBSV used to obtain the 2D arrays was diluted in sodium acetate 20 mM buffer, pH = 5.9, $MgCl_2$ 50 mM, $CaCl_2$ 10 mM. Solutions of viruses in the compact form were prepared with different concentrations from 0.1 to 0.4 mg/ml.

Ammonium molybdate solutions in the 5% to 10% concentration range were prepared as a condensing medium to promote the 2D crystallisation of the TBSV virus. Equal volume of diluted virus solutions and ammonium molybdate solutions are then mixed. A drop of 5 µl of the mixed solution is then deposited on a clean surface of a freshly cleaved mica sheet. The size of the sheet was 4x4 mm, *i.e.* a little larger than the diameter of the TEM grids. Electron microscopy grids were obtained by using the carbon replica technique. The transfer of the carbon replica was made on commercial 200 mesh copper grids.

Streptavidin 2D crystals were produced by modifying the protocol proposed by Scheuring *et al.* [19] : 50 µl of 10mM Tris-HCl, pH = 7.5, 150 mM NaCl buffer solution was injected in a Teflon well of 3.5 mm in diameter. A 0.5 µl of a lipid mixture containing Biotin-LC-DPPE (Long Chain – Dipalmitoyl-PhosPhatidyl-Ethanolamine) / DOPC (DioleOyl-Phosphatidyl-Choline) in 1 to 4 molar ratio and chloroform / hexane in 1 to 1 molar ratio was then deposited at the surface of the Teflon well to form the lipid monolayer (Fig 1a). From the lateral well, 5 µl of the solution was removed using a syringe and replaced by 5 µl of a solution containing the streptavidin at a concentration of 100 µg/ml. Incubation overnight at 4°C allowed the adsorption of protein to the lipid monolayer and subsequent growing of the 2D crystals. For TEM observations, the sample was negatively stained with 1% uranyl acetate solution and dried in air.

The 2D superlattices are then transferred to a high vacuum chamber in order to grow metal nanoparticles. The synthesis of Ag nanoparticles has been made by thermal evaporation. The

silver atoms are deposited at a pressure close to 10^{-8} mbar during evaporation. The source was a Knudsen type cell containing high purity Ag pellets heated at 990ºC. The typical deposition rate, measured by using a quartz balance, was 0.6 nm/min. The substrate (*i.e.* Cu grid and the 2D superlattices on carbon film) was held at room temperature. In order to stabilize the 2D superlattices of NPs, a 3 nm layer of amorphous Al_2O_3 was deposited *in situ* on the top of the film. The silver amount deposited onto the 2D lattices, also called nominal thickness, is equivalent to the thickness of a continuous layer. Here the nominal thickness was 0.75 nm and 0.3 nm on TBSV and streptavidin biotemplates respectively.

3. Results and discussion

3.1 *2D-organization of virus on mica surface*

Tomato Bushy Stunt Virus (TBSV) is a spherical plant virus that belongs to the family of Tombusviridae. The diameter of TBSV in the compact form is 32 nm (Fig. 2a) [20]. The evaporation of the drop containing TBSV and condensing medium (ammonium molybdate solution), can lead to the formation of TBSV 2D superlattices. The driving forces of viruses ordering are capillary forces at the fluid / air interfaces. The thermodynamic stability of self assembly of the viruses results in a competition between the shielding of the surface charges (*i.e.* the quantity of condensing medium) and the kinetic of the evaporation rate. Ammonium molybdate is a polar reagent which neutralizes the surface charges of the viruses. Therefore with an appropriate concentration of ammonium molybdate (see experimental section), self organization reaction occurs on the mica surface.

For 0.2 mg/ml TBSV concentration and 5% ammonium molybdate concentration, stable compact hexagonal structures are formed over large areas (Fig. 2b). Typical sizes of the self-organized domains are about a few microns (up to 10 µm). The unit cell parameter of the 2D crystal is imposed by the diameter of the virus and was measured to be 33.5 ± 0.5 nm on the power spectrum of the TEM image. This value is in very good agreement with the one

expected in case of a 2D close packed hexagonal superlattice constituted of spheres of 32 nm in diameter.

The evaporation kinetics was controlled by modifying the degree of humidity of the ambient conditions in which experiments were carried out. We have evidenced that the close packed hexagonal phase transform into a square structure for high evaporation rate. The square structure has the same unit cell parameter that the hexagonal structure (Fig. 2c) and can also be observed over several microns large areas. This phase transition emphasizes the high sensitivity of self assembly processes to external parameters, since a small increase of the kinetic of evaporation lead to the formation of a metastable structure with a non-compact 2D arrangement.

For intermediate evaporation rate, the structure of the 2D superlattices consists in a mixing of the hexagonal and square structures (Fig. 2d). The coexistence of the two phases induces the presence of disordered areas and many crystal defects. These latter are implied in the mechanisms of structural transformation between cubic and hexagonal structures. The same kind of transition is commonly observed in pure metals and alloys which exhibit phase transitions from face centred cubic to hexagonal 3D structures or the reverse [21].

By varying the virus concentration while keeping the same ammonium molybdate concentration, we change the surface charge of the viruses. It is then possible to modify the symmetries of the 2D superlattices. For 0.1 mg/ml TBSV concentration, oblique and open hexagonal superlattices are formed (Figs. 2e and 2f). The size of the organized domains is relatively small compared to the one obtained with the 0.2 mg/ml TBSV concentration : between 400 to 800 nm *vs* few microns. If these latter configurations cannot be considered as long-range ordered structures, they are very encouraging because their stabilisation over large areas would enhance the potential of TBSV for biotemplating. More particularly, the open hexagonal TBSV superlattice could then serve as a lithographic nano-mask.

3.2 *2D-organization of Ag nanoparticles on TBSV superlattices*

The 2D TBSV superlattices are then used as templates for the growth of metal nanoparticles. The growth of the particles is carried out by depositing metallic vapour phase under high vacuum condition by thermal evaporation. The growth was made at room temperature in order to avoid the alteration of the viruse shape and sub-nanometer nominal thickness was chosen in order to form separated cluster (see experimental section). Silver was chosen because it has a high surface mobility even at room temperature and the deposition rate was low to promote the organization of the NPs. We deposited Ag vapour phase on hexagonal (Fig. 3a) and square (Fig. 3b) TBSV superlattices. The silver atoms which come from the vapour phase are fixed on topographically or chemically privileged sites and form nanoparticles on the surface of the viruses. Braun *et al.* have shown the presence of such sites on enzymatic proteins [22]. On TBSV, at room temperature, the diffusion of Ag atoms is limited and the viruses act as barriers preventing the nucleation of additional clusters within the free space between the viruses. Therefore several Ag clusters are observed on each virus and form a decoration pattern. These decoration patterns reproduce the symmetry of the TBSV superlattice and their defects. It is therefore possible to easily observe the virus superlattice even on a non-stained sample. As an example, an edge dislocation is observed in the square superlattice on fig 3b.

The precise 3D shape of TBSV has been determined by Aramayo *et al.* [20] using cryo-electron microscopy (cryo-TEM) and single particle analysis technique. TBSV has a spherical overall shape with all the symmetries of the icosahedron (T3 icosahedral symmetry [20]). The capsid protein is formed by protruding domains exhibiting 5-fold (pentagonal) and 6-fold (hexagonal) symmetries. Consequently, the cavity at the center of a hexagon (or pentagon) is also at the center of a larger hexagon (pentagon) formed by the surrounding cavities. Figs. 3d and 3e show the projection of the TSBV along the 5- and 6-fold symmetry axes respectively. Each decoration pattern formed by the NPs is characteristic of the shape and orientation of the

underlying virus. Fig. 3c shows that the decoration patterns are mostly centred pentagon or centred hexagon. The comparison between the decoration patterns and 3D shape of the TBSV allow the identification of the nucleation sites which correspond to the cavities formed by protruding domains of the TBSV capsid. Ag nanoparticles are situated at the centre and the vertexes of a pentagon (in blue on fig. 3d) or a hexagon (in red on fig. 3e). The nanoparticle size varies from 3 to 5.5 nm which is in good agreement with the size of the cavities (~ 5.7 nm) and the inter-particle mean distance corresponds to the distance between these cavities. We note that there is significant interest in building such hybrid nanosystems which bridge the inter-particle distance, in order to exploit the interesting electron transport and optical phenomena present in 3-D assemblies of discrete metal nanoparticles. [23-25] On the one hand, this work demonstrates that vapour phase deposition experiments are an interesting approach to study TBSV, or other single molecules, with regard to their capsid symmetries, orientation and self-organization properties [22]. On the other hand, these results show that 2D self-organized TBSV can be used as a biotemplate to form under high vacuum conditions, long-range ordered decoration patterns of metallic particles. Nevertheless, due to the random orientation of the viruses on the substrate, the decoration patterns are not identical from a virus to another. Strictly speaking, even if the tuneable arrangements over long distance of TBSV are very interesting for biotemplating applications, perfectly periodic NPs patterns cannot be expected with such randomly oriented molecules. This limitation could be overcome by controlling the orientation of the viruses, which unfortunately remains challenging.

3.3 *2D-organization of Ag nanoparticles on streptavidin 2D crystals*

Proteins that are known to form perfect 2D crystals are very attracting fabrication platforms for templating ordered nanoparticle arrays [9-11]. For that purpose, we have selected the streptavidin proteins which easily form 2D crystals when deposited on flat surfaces.

Highly ordered streptavidin 2D crystals on biotinylated lipid monolayers are produced at the air/water interface [26] and are transferred, thanks to capillary forces, on a 400 mesh Cu TEM grids covered by a thin carbon film (Fig. 1a). A TEM bright field image of the 2D crystals in negative staining is shown in Fig. 4a. From the power spectrum of the image, shown in the inset, the mean distance between the streptavidin proteins is found to be 6.1 nm and consequently, the unit cell parameters of the centred square structure of streptavidin 2D crystal are: $a = b = 8.5 \pm 0.2$ nm and $\gamma = 90 \pm 1°$. These values are very close to the ones determined by Scheuring *et al.* using atomic force microscopy [19]. The streptavidin is a tetramer protein: it has 4 biotin bonding sites[11]. Two are occupied by linkage to the lipid layer and the two other are free and can be functionalized. For this purpose, Nanogold® labelling reagent from the Nanoprobes Inc. company was used. It consists in a reactive sulfo-N-hydroxy-succinimido functionality incorporated into a ligand on a 1.4 nm size diameter gold NP. The sulfo-N-hydroxy-succinimido chain has a specific reactivity towards primary amines and can form covalent bonds with any proteins bearing an accessible primary amine as it is the case for the streptavidin protein in our experimental conditions (fig. 1b).

The streptavidin / Nanogold® 2D crystals were transferred into the growth chamber and we used the same growth conditions as in the case of TBSV. The Nanogold plays the role of seeds for the growth of Ag NPs resulting in the formation of the 2D organized superlattice. This method is very efficient since the particles reproduced very well the underlying symmetry of the protein 2D crystal (Fig. 4b). Indeed, the same square symmetry is observed on the power spectrum of the images 4a and 4b, which correspond to the stained-streptavidin 2D crystal and the NPs superlattice, respectively. Then, the mean distance between particles is only 6.1 nm. The degree of order of the NP arrays relative to that of the underlying biotemplate is actually much better than previously reported [11,27]. This result highlights the efficiency of chemical adsorption of the Nanogold® labelling reagent on the streptavidin 2D crystal. Energy dispersive X-ray analysis confirmed the presence of both silver and gold in the

NPs. The mean size of the particles is 3.8 ± 0.4 nm. This size distribution is very narrow (10 % polydispersity) compared to standard growth of nanoparticles by thermal evaporation on amorphous substrate (from 30 to 50 % polydispersity depending on growth condition) [9-11]. Up to now, only post-synthesis flash laser annealings [28] or chemical synthesis [3] allow the fabrication of such monodisperse metallic NPs. This NP feather is commonly observed when vapour phase deposition techniques are performed on a substrate with a periodic distribution of privileged sites for the nucleation [4,29]. In these nanofabrication experiments, there is a correlation between cluster spacing and cluster size [30]. Indeed, silver atoms deposited onto the area closest to a gold seed are likely to attach to this seed. This capture area is called the Voronoi polygon of the seed. As the gold seed are equidistant to each other, their Voronoi areas are identical thus leading to very narrow NPs size distribution. Further works are in progress to understand and avoid the formation of the largest NPs observed on image 4b. As on TBSV the ordered domains are about a micron large, but this time the obtained square pattern is perfectly periodic. Therefore, streptavidin / Nanogold® 2D crystals offer a new opportunity to control both the size and 2D-organization of inorganic NPs below the 10 nm scale.

4. Conclusion

In this paper, we demonstrate how the use of biochemistry and physical approaches can lead to the fabrication of 2D superlattices of metallic NPs. The mechanisms driving such organized growth are all based on heterogeneous nucleation. The growth of 3D metal NPs requires a two-dimensional mobility of atoms on the surface. As long as the energy of absorption is larger than the energy of activation of diffusion, atoms can diffuse over large distances at a given temperature. On a perfectly uniform surface, the metal atoms diffuse until meeting other atoms or existing NPs. They can then growth to form bigger stable particles randomly distributed on the surface: this is the homogeneous nucleation mechanism. Conversely, in

inhomogeneous nucleation, defects on the surface which have higher energy of adsorption are privileged sites for the nucleation.

In the case of viruses, nucleation takes place in the capsid cavities, whereas on streptavidin 2D crystals the nucleation sites are formed by grafting very small nanogold particles on the streptavidin proteins during the preparation of the 2D crystal. Ag nanoparticles are then formed under high vacuum conditions by thermal evaporation process. All these 2D lattices of nanoparticles can be protected from alteration by depositing a thin layer of amorphous materials and can then be used for fundamental studies or applications since there are stable over long period of time.

Acknowledgements

We are grateful to Region Ile-de-France for convention SESAME 2000 E1435, for the support of the JEOL 2100F electron microscope installed at IMPMC (UMR 7590).

References

(1) Nahas, Y.; Repain, V.; Chacon, C.; Girard, Y.; Lagoute, J.; Rodary, G.; Klein, J.; Rousset, S.; Bulou, H.; Goyhenex, C. *Physical Review Letters* **2009**, *103*, 067202.

(2) Taleb, A.; Petit, C.; Pileni, M. P. *Journal of Physical Chemistry B* **1998**, *102*, 2214-2220.

(3) Motte, L.; Billoudet, F.; Pileni, M. P. *The Journal of Physical Chemistry* **1995**, *99*, 16425-16429.

(4) Repain, V.; Rohart, S.; Girard, Y.; Tejeda, A.; Rousset, S. *Journal of Physics-Condensed Matter* **2006**, *18*, S17-S26.

(5) Sotiropoulou, S.; Sierra-Sastre, Y.; Mark, S. S.; Batt, C. A. *Chemistry of Materials* **2008**, *20*, 821-834.

(6) Zhang, J.; Liu, Y.; Ke, Y.; Yan, H. *Nano Letters* **2006**, *6*, 248-251.

(7) Flynn, C. E.; Lee, S.-W.; Peelle, B. R.; Belcher, A. M. *Acta Materialia* **2003**, *51*, 5867-5880.

(8) Yamashita, I.; Iwahori, K.; Kumagai, S. *Biochimica Et Biophysica Acta-General Subjects* **2010**, *1800*, 846-857.

(9) McMillan, R. A.; Paavola, C. D.; Howard, J.; Chan, S. L.; Zaluzec, N. J.; Trent, J. D. *Nat Mater* **2002**, *1*, 247-252.

(10) Shenton, W.; Pum, D.; Sleytr, U. B.; Mann, S. *Nature* **1997**, *389*, 585-587.

(11) Shindel, M. M.; Mumm, D. R.; Wang, S.-W. *Langmuir*, *26*, 11103-11112.

(12) Langlois, C.; Alloyeau, D.; Le Bouar, Y.; Loiseau, A.; Oikawa, T.; Mottet, C.; Ricolleau, C. *Faraday Discussions* **2008**, *138*, 375 - 391.

(13) Alloyeau, D.; Langlois, C.; Ricolleau, C.; Le Bouar, Y.; Loiseau, A. *Nanotechnology* **2007**, *18*, 375301.
(14) Alloyeau, D.; Ricolleau, C.; Mottet, C.; Oikawa, T.; Langlois, C.; Le Bouar, Y.; Braidy, N.; Loiseau, A. *Nature Materials* **2009**, *8*, 940-946.
(15) Alloyeau, D.; Ricolleau, C.; Oikawa, T.; Langlois, C.; Le Bouar, Y.; Loiseau, A. *Ultramicroscopy* **2008**, *108*, 656-662.
(16) Harris, J. R. *J Electron Microsc Tech* **1991**, *18*, 269-76.
(17) Harris, J. R.; Gebauer, W.; Guderian, F. U.; Markl, J. *Micron* **1997**, *28*, 31-41.
(18) Harris, J. R.; Scheffler, D. *Micron* **2002**, *33*, 461-80.
(19) Scheuring, S.; Muller, D. J.; Ringler, P.; Heymann, J. B.; Engel, A. *J. Microsc.* **1999**, *193*, 28-35.
(20) Aramayo, R.; Mérigoux, C.; Larquet, E.; Bron, P.; Pérez, J.; Dumas, C.; Vachette, P.; Boisset, N. *Biochimica et Biophysica Acta (BBA) - General Subjects* **2005**, *1724*, 345-354.
(21) Dureuil, V.; Ricolleau, C.; Gandais, M.; Grigis, C. *The European Physical Journal D - Atomic, Molecular, Optical and Plasma Physics* **2001**, *14*, 83-88.
(22) Braun, N.; Meining, W.; Hars, U.; Fischer, M.; Ladenstein, R.; Huber, R.; Bacher, A.; Weinkauf, S.; Bachmann, L. *Journal of Molecular Biology* **2002**, *321*, 341-353.
(23) Blum, A. S.; Soto, C. M.; Wilson, C. D.; Cole, J. D.; Kim, M.; Gnade, B.; Chatterji, A.; Ochoa, W. F.; Lin, T. W.; Johnson, J. E.; Ratna, B. R. *Nano Letters* **2004**, *4*, 867-870.
(24) Li, T.; Niu, Z. W.; Emrick, T.; Russell, T. R.; Wang, Q. *Small* **2008**, *4*, 1624-1629.
(25) Wang, Q.; Lin, T. W.; Tang, L.; Johnson, J. E.; Finn, M. G. *Angewandte Chemie-International Edition* **2002**, *41*, 459-462.
(26) Blankenburg, R.; Meller, P.; Ringsdorf, H.; Salesse, C. *Biochemistry* **1989**, *28*, 8214-8221.
(27) Shindel, M. M.; Mohraz, A.; Mumm, D. R.; Wang, S.-W. *Langmuir* **2008**, *25*, 1038-1046.
(28) Alloyeau, D.; Ricolleau, C.; Langlois, C.; Le Bouar, Y.; Loiseau, A. *Beilstein Journal of Nanotechnology* **2010**, *1*, 55-59.
(29) Renard, C.; Ricolleau, C.; Fort, E.; Besson, S.; Gacoin, T.; Boilot, J. P. *Applied Physics Letters* **2002**, *80*, 300-302.
(30) Mulheran, P. A.; Blackman, J. A. *Physical Review B* **1996**, *53*, 10261.

Figures:

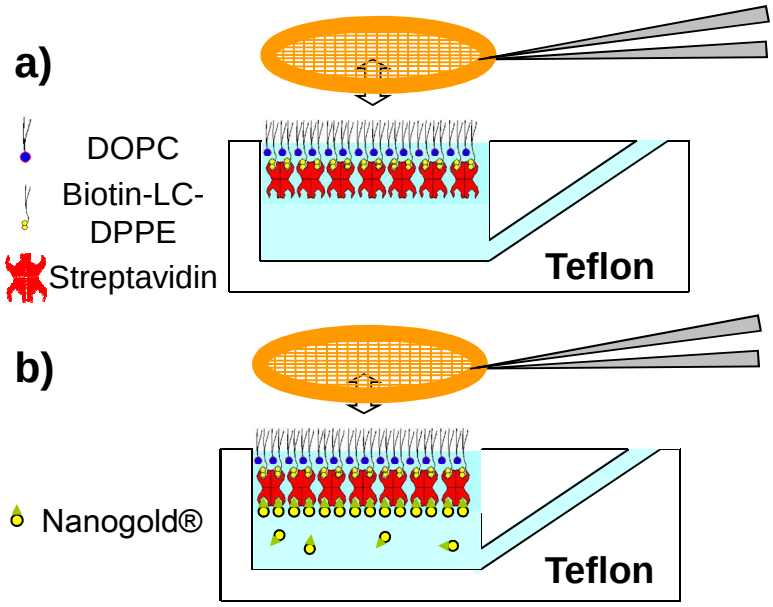

Fig. 1: Schematic representations. (a) Formation of the 2D streptavidin lattices on biotinylated lipid monolayers. (b) Grafting of the streptavidin with Nanogold®.

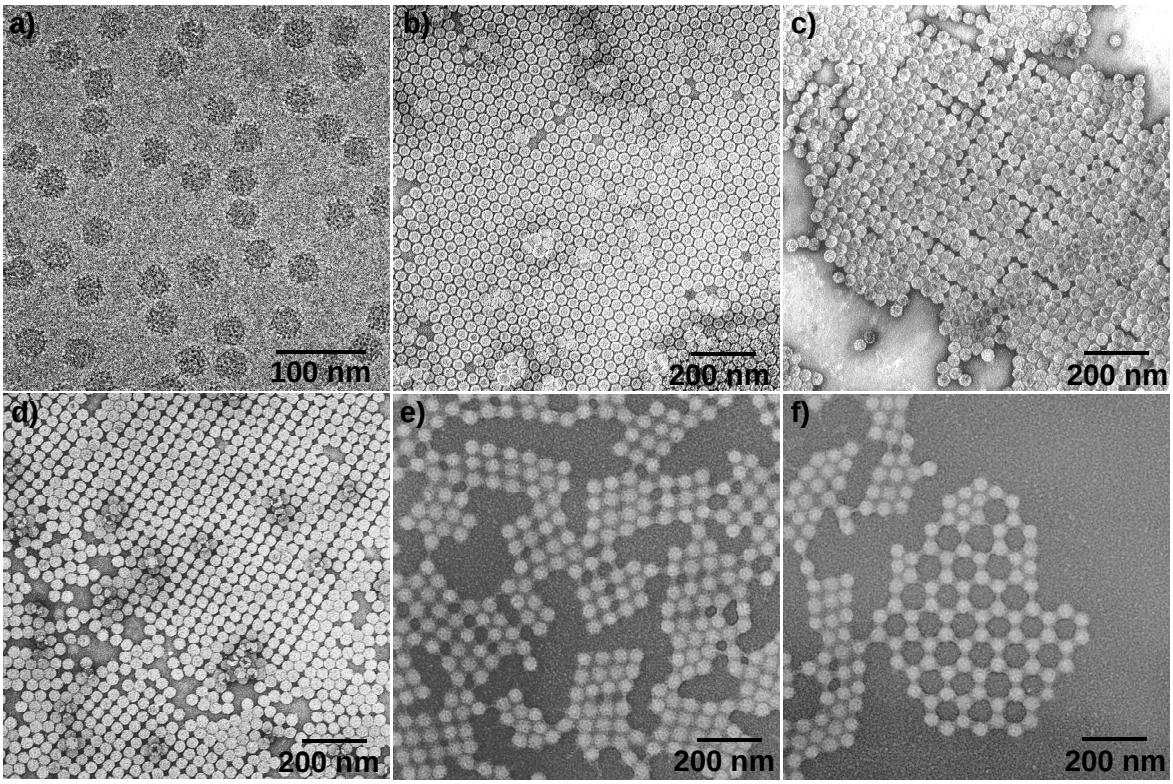

Fig. 2: (a) TEM bright field image of TBSV viruses observed in cryo-electron microscopy [20]. 2D superlattices formed by using a 0.2 mg/ml TBSV concentration : (b) hexagonal and (c) square 2D superlattices obtained with ammonium molybdate as a condensing medium. (d)

Coexistence of the two structures exhibiting stacking faults. 2D superlattices formed by using a 0.1 mg/ml TBSV concentration : (e) oblique and (f) open hexagonal 2D superlattices

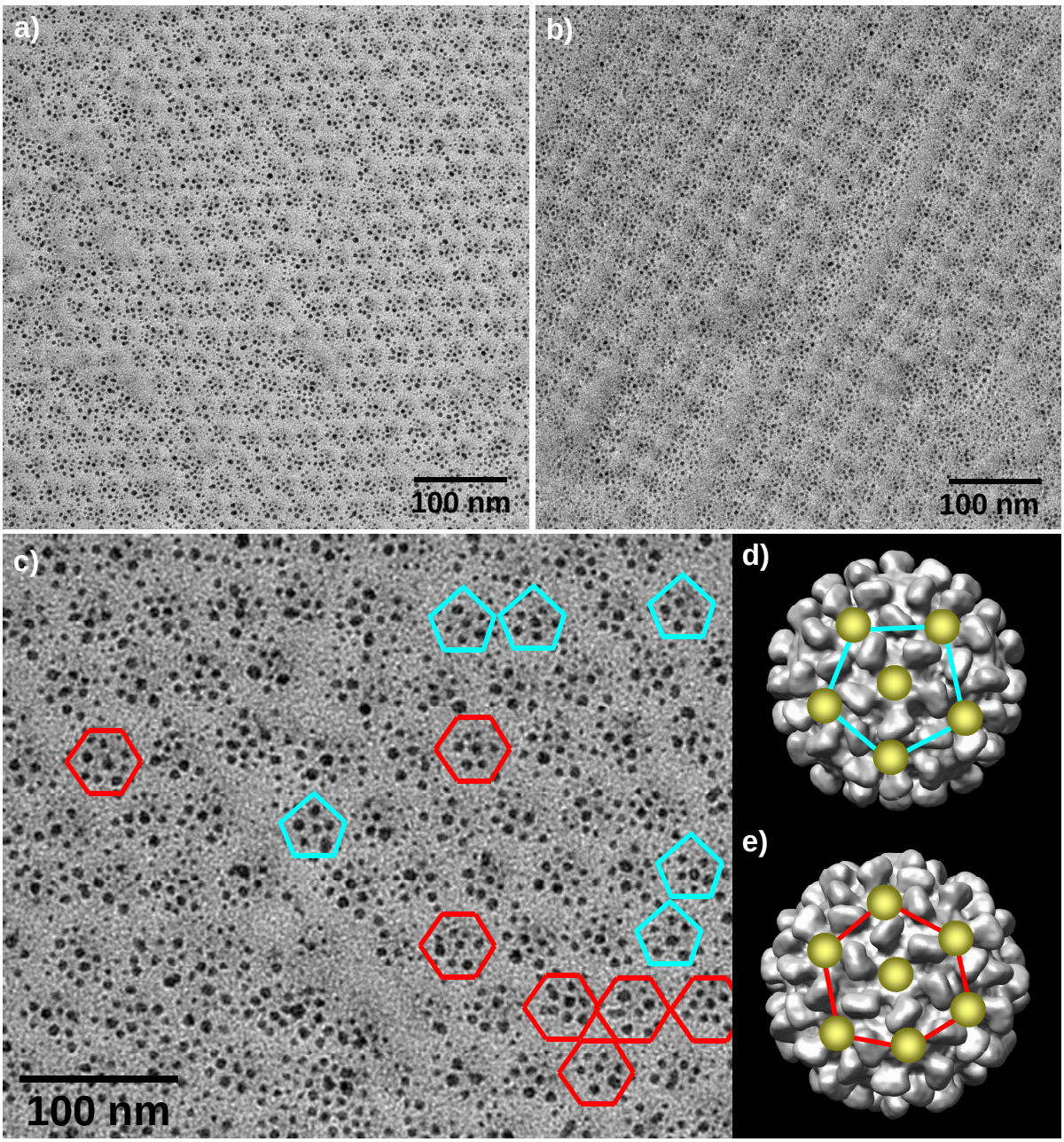

Fig. 3: TEM bright field images of the decoration patterns obtained with 0.75 nm in nominal thickness of Ag deposited on 2D TSBV : (a) hexagonal and (b) square superlattices. (c) Identification of the nucleation site of Ag NPs : the centred hexagonal and centred pentagonal decoration patterns of particles are highlighted in red and blue respectively. Projections of the

TBSV along the (d) 5-fold axis and (e) 6-fold axis showing the nucleation sites of the Ag NPs which correspond to the cavities of the virus capsid.

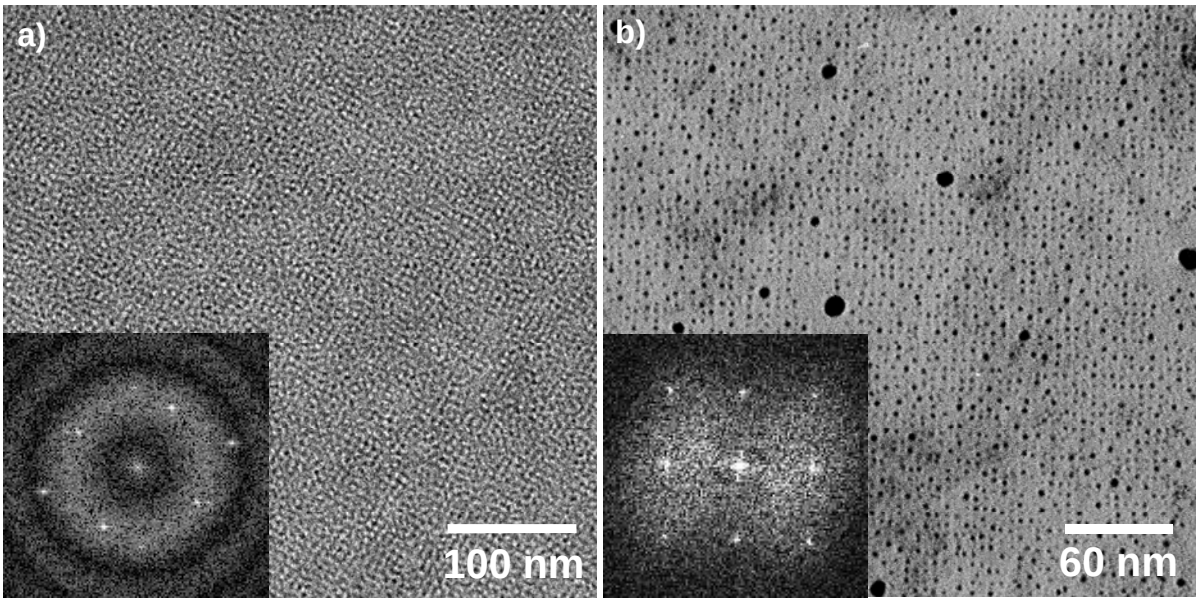

Fig. 4: (a) TEM bright field image of the streptavidin in negative staining (inset : power spectrum of the image). (b) 2D superlattices of Ag NPs obtained by depositing 0.3 nm in nominal thickness of Ag on a 2D streptavidin / Nanogold® lattice.

TOC graphic